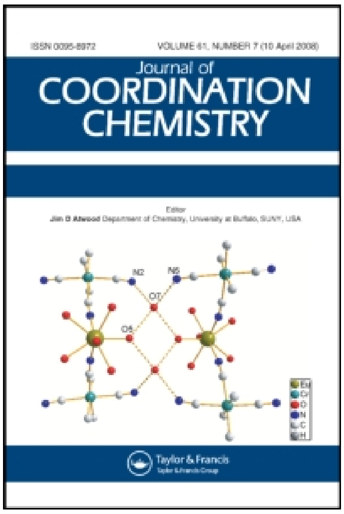

Journal of Coordination Chemistry
Publication details, including instructions for authors and subscription information:
http://www.informaworld.com/smpp/title~content=t713455674

THE PHENOMENON OF CONGLOMERATE CRYSTALLIZATION. XXVII. THE EFFECT OF CHARGE COMPENSATING ANION ON THE CRYSTALLIZATION BEHAVIOUR OF [Co(en)$_2$ox]-Cl·4H$_2$O, [Co(en)$_2$ox]Br·H$_2$O, [Co(en)$_2$ox]PF$_6$ AND [Co(en)$_2$ox]I

Ivan Bernal[a]; James Cetrullo[a]; Jozef Myrczek[ab]; Salah S. Massoud[c]
[a] Department of Chemistry, University of Houston, Houston, Texas, U.S.A. [b] Technical University of Wroclaw, Wroclaw, Poland. [c] Chemistry Department, Faculty of Science, University of Alexandria, Alexandria, Egypt

To cite this Article Bernal, Ivan , Cetrullo, James , Myrczek, Jozef and Massoud, Salah S.(1993) 'THE PHENOMENON OF CONGLOMERATE CRYSTALLIZATION. XXVII. THE EFFECT OF CHARGE COMPENSATING ANION ON THE CRYSTALLIZATION BEHAVIOUR OF [Co(en)$_2$ox]-Cl·4H$_2$O, [Co(en)$_2$ox]Br·H$_2$O, [Co(en)$_2$ox]PF$_6$ AND [Co(en)$_2$ox]I', Journal of Coordination Chemistry, 30: 1, 29 — 51

To link to this Article: DOI: 10.1080/00958979308022745

URL: http://dx.doi.org/10.1080/00958979308022745

J. Coord. Chem., 1993, Vol 30, pp. 29–51
Reprints available directly from the publisher
Photocopying permitted by license only

THE PHENOMENON OF CONGLOMERATE CRYSTALLIZATION. XXVII. THE EFFECT OF CHARGE COMPENSATING ANION ON THE CRYSTALLIZATION BEHAVIOUR OF $[Co(en)_2ox]Cl{\cdot}4H_2O$, $[Co(en)_2ox]Br{\cdot}H_2O$, $[Co(en)_2ox]PF_6$ AND $[Co(en)_2ox]I$

IVAN BERNAL,* JAMES CETRULLO, JOZEF MYRCZEK†

Department of Chemistry, University of Houston, Houston, Texas 77204-6541, U.S.A.

SALAH S. MASSOUD*

Chemistry Department, Faculty of Science, University of Alexandria, P.O. Box 428, Alexandria 21321, Egypt

(Received 21 September 1992)

$[Co(en)_2ox]Cl{\cdot}4H_2O$ (I) and $[Co(en)_2ox]Br{\cdot}H_2O$ (II), crustallize from water at 21°C as conglomerates, space group $P2_12_12_1$. Their structures and absolute configurations were determined by refinement of data using both enantiomeric configurations. $[Co(en)_2ox]PF_6$ (III) crystallizes as a racemate, space group $P2_1/c$. $[Co(en)_2ox]I$ (IV) crystallizes in both of the monoclinic space groups $C2$ and $C2/c$, in agreement with the phase diagram studies of Yamanari, *et al.* (see ref. 4). However, we have not been successful in crystallographic studies of this substance since in neither case was it possible to obtain ordered crystals.

The conglomerate crystallization pathway selected by (I) and (II), and probably (IV), is shown to be the result of inter-cationic, three-point attachments reminiscent of that postulated as the origin of enzymatic chiral recognition. In this process, spiral strings are formed which resemble polypeptide helices, and which are stitched together by the counternions (and/or waters of crystallization, where relevant) such that each crystal contains, exclusively, homochiral strings of one helicity.

KEY WORDS: Conglomerate crystallization, racemates, ordered crystals, disordered crystals, mechanisms of crystallization, metal amines, metal oxalates.

INTRODUCTION

We have recently determined the structure and absolute configuration[1] of the amine oxalato Co(III) complex $[Co(NH_3)_4ox]NO_3.H_2O$ (V), which crystallizes as a conglomerate (homochiral crystals), space group $P2_12_12_1$. Its iodide analogue, $[Co(NH_3)_4ox]I.H_2O$ (VI) crystallizes as a racemate (heterochiral crystals), space group $P2_1/n$, and we provided[1] a rationalization of this difference in crystallization as being

---

* Authors for correspondence.
† On leave from the Technical University of Wroclaw, 1-5 Wroclaw, Poland.

the result of inter-ionic hydrogen bonding which locks (V) in a dissymmetric configuration stable enough to influence the outcome. The reader is referred to the original for more details. Also, it has been known for some time that $[Co(en)_2ox]X$ ($X = Cl{\cdot}4H_2O$, $Br{\cdot}H_2O$),[2-6] $[Cr(en)_2ox]X$ (X = Cl, Br)[2-5] and $[Rh(en)_2ox]Br$[5] crystallize as conglomerates, but that $[Co(en)_2ox]I$ crystallizes as both a conglomerate and a racemate.[4] Coudwell *et al.*[7] reported that *mer*-$[Co(dien)(NH_3)ox]NO_3$, forms crystalline conglomerates whereas its PF_6-analogue crystallizess as a racemate—a fact we justified,[1] again, on the basis of inter-molecular bonding between nitrate and the amine hydrogens. Additionally, $K_3[Co(ox)_3]{\cdot}H_2O$ was shown by Jaeger and Thomas[8] and by Tutton[9] to crystallize as a conglomerate when the crystallization temperature is 13.2°C. The structure and absolute configuration of a pre-resolved sample of $(-)_{589}$-$[Co(en)_2ox]Br{\cdot}H_2O$ was determined[6] using a very limited amount of film data.

In as much as many of the compounds of the amine oxalato series are prone to crystallize as conglomerates, and that the crystallization pathway seems to be influenced by the choice of counter anion, it seemed reasonable to carry out a more systematic effort to understand why this is so; moreover, we wanted, if possible, to attach a molecular reason for this behaviour. Therefore, since the crystal structures of the series $[Co(en)_2ox]X{\cdot}yH_2O$ (X = Cl, y = 4; X = Br, y = 1; X = PF_6, y = 0; X = I, y = 0) were unknown in the case of the chloride, the iodide and the hexafluorophosphate, we decided to explore the structures of all four compounds in the hope of producing some evidence for the difference in crystallization mode within the halide series. The hexafluorophosphate was also studied since its anion should be as bulky, and a similar hydrogen bonding anion, as iodide. Moreover, we hoped a comparison of the crystallization behaviour of the halide series would also be enlightening as to the effect of progressively increasing anionic bulk on the crystallization pathway of these cations.

EXPERIMENTAL

Syntheses

Compound (**I**) was prepared as follows: the synthetic procedure of Bailar[10] for the preparation of [trans-$Co(en)_2Cl_2]Cl{\cdot}HCl$ was used, and the product converted to *cis*-$[Co(en)_2Cl_2]Cl$ as described by him;[10] 0.1 mol of *cis*-$[Co(en)_2Cl_2]Cl$ was stirred with 150 cm^3 of water, the temperature raised to 60° and 0.1 mol of solid ammonium oxalate slowly added. Shortly, the solution changed from blue-purple to orange-red and was allowed to cool to room temperature, filtered and set aside for crystals to grow. Slow evaporation of the mother liquor produced the desired crystals of (**I**). These crystals rapidly effloresce if not in contact with mother liquor, and crumble to a fine powder in less than two hours. Therefore they were placed in capillaries with a drop of mother liquor in order to collect X-ray data.

Compounds (**II**), (**III**) and (**IV**) were obtained from saturated solutions of (**I**) which were treated with an excess of either NaBr, NaI or NH_4PF_6. Solutions of the salts thus obtained were allowed to evaporate at room temperature. The bromide is a monohydrate and the iodide and hexafluorophosphate are anhydrous. Unlike the chloride, crystals of the bromide iodide and hexafluorophosphate derivatives are stable in the open air, indefinitely.

Elemental Analyses

Elemental analyses for (**I**), (**II**) and (**III**) were not carried out since these are well-defined substances whose compositions were aleady established.[4,10] Elemental analysis of the hexafluorophosphate was carried out at the Elemental and Microanalytical Laboratory of Ciba-Geigy, Switzerland, whom we thank for their courtesy. Theory for $CoPF_6O_4N_4C_6H_{16}$: % C, H, N, Co = 17.49, 3.91, 13.60, 14.30. Exp: 17.63, 3.73, 13.47, 14.51.

Crystallography

Data were collected with an Enraf-Nonius CAD-4 diffractometer operating with a Molecular Structure Corporation TEXRAY-230 modification[11] of the SDP-Plus software package.[12] The procedure used for crystal alignment, cell constant determination, space group determination, and data collection was uniform for all three crystals. They were centred with data in the $20° \leqslant 2\Theta \leqslant 34°$ range and examination of the cell constants, absences, and Niggli matrix[13] clearly showed (**I**) and (**II**) to crystallize in a primitive, orthorhombic space group whose systematic absences identify it as $P2_12_12_1$. Compound (**III**) crystallizes in a primitive, monoclinic lattice. Systematic absences clearly show the presence of a two-fold screw axis and an *c*-glide; thus, its space group is unequivocally $P2_1/c$. Compound (**IV**) appears to crystallize alternately in space groups *C*2 and *C*2/*c*. Both crystals are of poor quality, the latter being the worst, with both disordered to different degrees. Both display variable peak widths. The cell obtained for the *C*2 sample indexed in a reasonble fashion; however, in order to obtain a cell for the *C*2/*c* sample, we had to edit the reflection file repeatedly until we obtained a non-singular matrix. The reader is warned of the preliminary nature of these results.

The details of data collection are summarized in Tables 1, 2, 3 and 4, respectively, for compounds (**I**), (**II**), (**III**), and (**IV**). The intensity data sets were corrected for absorption using empirical curves derived from Psi scans[11,12] of suitable reflections. the scattering curves were taken from Cromer and Waber's compilation.[14] During data collection with (**I**), the crystal moved inside the capillary after collecting 2300 reflexions. Data collection was terminated by the diffractometer since the intensity standards suddenly fell to less than 80% of the original. Telescopic examination of the crystal verified that it no longer was in the centre of the cross hairs; therefore, since the data set was nearly complete, data collection was terminated and all reflections past the last set of stable standards were eliminated from the data set. Data collection for (**II**) and (**III**) was straightforward. Data collection for (**IV**), in space group *C*2, seemed reasonable until we solved the structure and found it disordered at the ethylenediamine rings. No data were collected with the *C*2/*c* specimen.

The structures of (**I**) and (**III**) were solved from their Patterson maps, using the Co atom as the heavy atom. For compounds (**II**) and (**IV**), the heavy atoms were Br and I, respectively. The Patterson function for (IV) and the distribution of intensities (Roger's Test)[11,12] suggested the correct space group was the acentric one, *C*2. Therefore, we selected it for the solution and refinement. The choice of *Cm* and *C*2/*m* produced no meaningful results. After refinement of the scale factor and the positional parameters of the heavy atoms, a difference Fourier map produced, in the other three cases, many of the non-hydrogen atoms. The remaining atoms were found in subsequent difference maps. Heavy atoms were refined isotropically until convergence, at which point the hydrogen atoms of the cations were added at idealized positions

Table 1 Summary of data collection and processing parameters for conglomerate $[Co(en)_2ox]Cl{\cdot}4H_2O$

Space Group	$P2_12_12_1$
Cell Constants	$a=6.349(3)$Å $b=11.969(4)$Å $c=20.311(5)$Å
Cell Volume	$V=1543.43$Å^3
Molecular Formula	$CoClO_8N_4C_6H_{24}$
Molecular Weight	374.67
Density (calc; $Z=4$ mol/cell)	1.630 g cm^{-3}
Radiation Employed	MoK$_\alpha$ ($\lambda=0.71073$Å)
Absorption Coefficient	$\mu=13.35$ cm^{-1}
Relative Transmission Coefficients	0.7293 to 0.9940
Data Collection Range	$4^\circ \leqslant 2\Theta \leqslant 60^\circ$
Scan Width	$\Delta\Theta=0.95+0.35\tan\Theta$
Total Data Collected	2300
Data Used In Refinement*	1583
$R=\sum\|\|F_o\|-\|F_c\|\|/\sum\|F_o\|$	0.048
$R_w=[\sum w^2(\|F_o\|-\|F_c\|)^2/\sum\|F_o\|^2]^{1/2}$	0.053
Weights Used	$w=[\sigma(F_o)]^{-2}$

*The difference between this number and the total is due to subtraction of 717 systematically absent reflections, redundant data collected to obtain reflections suitable for the absorption correction, ones which were symmetry related, standards or did not meet the criterion that $I \geqslant 3\sigma(I)$. Data collection was terminated early due to motion of the crystal in the capillary (see text).

Table 2 Summary of data collection and processing parameters for coglomerate $(-)589$-$\Delta(\delta\lambda)$-$[Co(en)_2ox]Br{\cdot}H_2O$

Space Group	$P2_12_12_1$
Cell Constants	$a=16.581(7)$Å $b=12.376(2)$Å $c=6.109(3)$Å
Cell volume	$V=1253.55$Å^3
Molecular Formula	$CoBrO_5N_4C_6H_{18}$
Molecular Weight	365.08
Density (calc; $Z=4$ mol/cell)	1.928 g cm^{-3}
Radiation Employed	MoK$_\alpha$ ($\lambda=0.71073$Å)
Absorption Coefficient	$\mu=42.24$ cm^{-1}
Relative Transmission Coefficients	0.7538 to 0.9998
Data Collection range	$4^\circ \leqslant 2\Theta \leqslant 70^\circ$
Scan Width	$\Delta\Theta=1.00+0.35\tan\Theta$
Total Data Collected	4150
Data Used In Refinement*	2949
$R=\sum\|\|F_o\|-\|F_c\|/\sum\|F_o\|$	0.042
$RR_w=[\sum w^2(\|F_o\|-\|F_c\|)^2/\sum\|F_o\|^2]^{1/2}$	0.050
Weights Used	$w=[\sigma(F_o)]^{-2}$

*The difference between this number and the total is due to subtraction of 2201 systematically absent reflections, redundant data collected to obtain reflections suitable for the absorption correction, ones which were symmetry related, standards or did not meet the criterion that $I \geqslant 3\sigma(I)$.

(N—H, C—H = 0.95Å) and all atoms were allowed to refine with hydrogen thermal parameters fixed at 5.0Å^2. Conversion of the heavy atoms to anisotropic motion resulted in refinement of the overall structure to final $R(F)$ and $R_w(F)$ factors listed in Tables 1 to 4, which summarize other details of data collection and processing.

Table 3 Summary of data collection and processing parameters for racemic $[Co(en)_2ox]PF_6$

Space Group	$P2_1/c$
Cell Constants	$a=8.701(3)Å$ $b=12.330(2)Å$ $c=12.676(3)Å$ $\beta=90.35(2)°$
Cell Volume	$V=1359.80Å^3$
Molecular Formula	$CoPF_6O_4H_4C_6H_{16}$
Molecular Weight	412.12
Density (calc; $Z=4$ mol/cell)	$2.013\ g\ cm^{-3}$
Radiation Employed	MoK_α ($\lambda=0.71073Å$)
Absorption Coefficient	$\mu=14.67\ cm^{-1}$
Relative Transmission Coefficients	0.8794 to 0.9996
Data Collection Range	$4° \leqslant 2\Theta \leqslant 50°$
Scan Width	$\Delta\Theta=1.00+0.35\tan\Theta$
Total Data Collected	2636
Data Used In Refinement*	1509
$R=\sum\|\|F_o\|-\|F_c\|\|/\|F_o\|$	0.084
$R_w=[\sum w^2(\|F_o\|-\|F_c\|)^2/\sum\|F_o\|^2]^{1/2}$	0.099
Weights Used	$w=[\sigma(F_o)]^{-2}$

*The difference between this number and the total is due to subtraction of 1127 systematically absent reflections, redundant data collected to obtain reflections suitable for the absorption correction, once which were symmetry related, standards or did not meet the criterion that $I \geqslant 3\sigma(I)$.

Table 4 Data available for enantiomorphic, disordered $[Co(en)_2ox]I$

Space Group	$C2$
Cell Constants	$a=11.915(3)Å$ $b=8.608(3)Å$ $c=7.474(1)Å$ $\beta=128.89(2)°$
Cell Volume	$V=596.72Å^3$
Molecular Formula	$ICoO_4N_4C_6H_{16}$
Molecular Weight	394.06
Density (calc; $Z=2$ mol/cell)	$2.193\ g\ cm^{-3}$
Radiation Employed	MoK_α ($\lambda=0.71073Å$)
Data Collection Range	$4° \leqslant 2\Theta \leqslant 50°$
Scan Width	$\Delta\Theta=1.00+0.35\tan\Theta$
Total Data Collected	822
Data Used In Refinement	421
$R=\sum\|\|F_o\|-\|F_c\|\|/\sum\|F_o\|$	0.22
Weights Used	$w=[\sigma(F_o)]^{-2}$

In the case of (**IV**), Table 4 lists only the space group and cell constants of the enantiomorphic phase crystallizing in space group $C2$.

*Absolute Configurations of (**I**) and of (**II**)*

The structure and absolute configuration of (**I**) was determined with a data set complete up to 47° (a total of 1363 data with $I \geqslant 3.0\sigma(I)$) at which point the $R(F)$ and $R_w(F)$ factors for the $(+\ +\ +)$ and $(-\ -\ -)$ coordinates were, respectively, (0.045 and

0.060) and (0.0530 and 0.065); thus, the original coordinates were selcted as being correct. When data collection was terminated due to the crystal moving, the refinement was completed with the new data set (1583 data with $I \geqslant 3.0\sigma(I)$). Convergence occurred with $R(F)$ and $R_w(F)$ factors of 0.048 and 0.053, respectively. In the case of (**II**) the refinement of the $(+++)$ structure converged at $R(F)=0.060$ and $R_w(F)=0.067$; those of the $(---)$ configuration, 0.042 and 0.050. Thus the latter was chosen, and its chiroptical symbol is $\Delta(\lambda\delta)$-[Co(en)$_2$ox]Br$\cdot$H$_2$O. Since our crystal was randomly selected from the crystalline mass, this result is accidentally in agreement with the conclusions of Aoki *et al.*[6] who used resolved crystals and characterized by them as being $(-)_{589}$-$\Delta(\lambda\delta)$-[Co(en)$_2$ox]Br$\cdot$H$_2$O (thus the assignment given in the title); also, since the counteranion should have no influence on the chiroptical sign of the cation, we assigned to the randomly selected crystal of the chloride the chiroptical symbol $(-)_{589}$-$\Delta(\lambda\delta)$-[Co(en)$_2$ox]Cl$\cdot$4H$_2$O on the basis of a comparison of the absolute configuration of the cations of the chloride and of the bromide, which accidentally share the same chiral symbols.

Figures 1 to 3 give labelled views of the contents of the asymmetric units of molecules of (**I**), (**II**) and (**III**). Their relative positions in the lattice were selected so as to be at the positions of strongest hydrogen bonds to their neighboring species. Figures 4 to 7 depict the packing of the ions (and water) in their respective unit cells. Care was exercised to have a common labelling scheme for all three cations; e.g., in

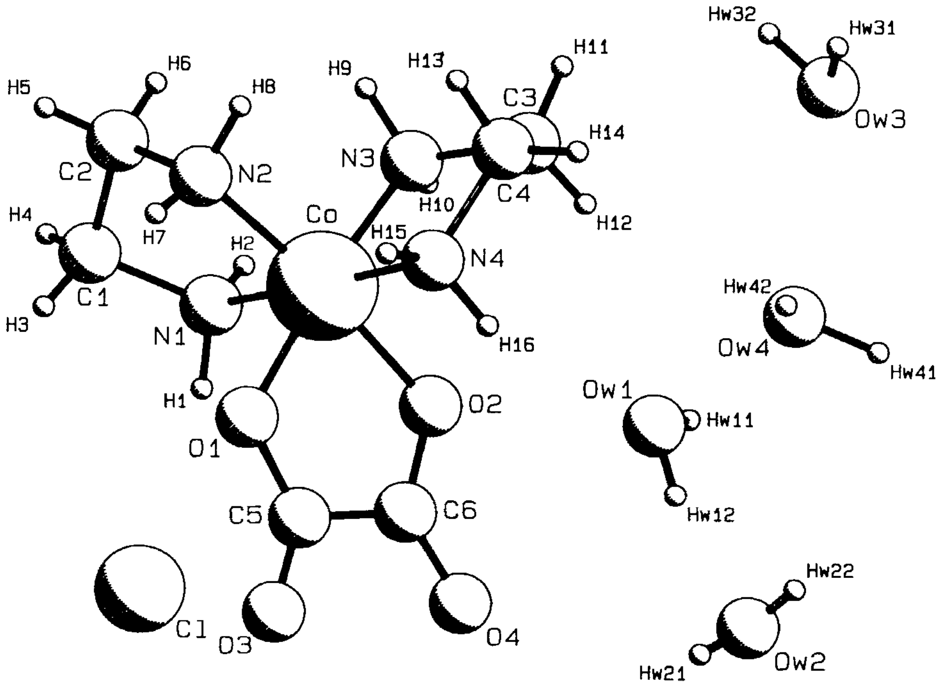

Figure 1 The contents of the asymmetric unit of compound (**I**) and the labelling system used in numbering the atoms present therein. The anion and the water of crystallization were placed at the crystallographic positions nearest to the cations insofar as hydrogen bonded interactions are concerned.

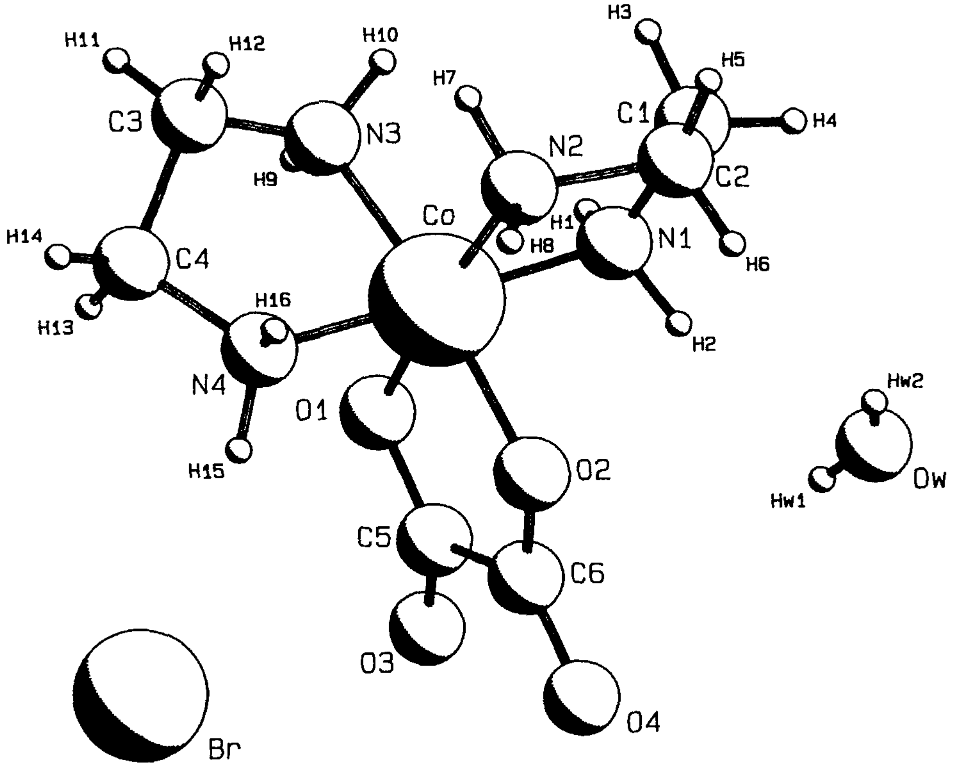

Figure 2 The contents of the asymmetric unit of compound (II) and the labelling system used in numbering the atoms present therein. The anion and the water of crystallization were placed at the crystallographic positions nearest to the cations insofar as hydrogen bonded interactions are concerned.

all cases N1 and N4 are at axial positions of the cobalt octahedron, N2 and N3 are at equatorial positions, O1 and O2 bind the Co, etc. Final positional and equivalent-isotropic thermal parameters are given in Tables 5 to 7. Bond lengths, angles and torsional angles are given in Tables 8 to 10. The anisotropic thermal parameters of the heavy atoms, as well as the structure factor tables for compounds (I) to (III) are available as Supplementary Material.

RESULTS AND DISCUSSION

The contents of the asymmetric units of compounds (I), (II) and (III) are shown in Figures 1 to 3 in order to establish the conformation and configuration of the cations present, as well as to record the atomic labelling system used in these studies. These drawings, along with the numerical data on Tables 5 to 7 allow us to establish the fact that the absolute configuration of the cations of (I) and (II) have the chiroptical symbols $\Delta(\lambda\delta)$-$[Co(en)_2ox]Cl \cdot 4H_2O$ and $\Delta(\lambda\delta)$-$[Co(en)_2ox]Br \cdot H_2O$. The chiroptical symbol for cation described by the coordinates (Table 3) of the racemate (III) is $\Lambda(\delta\delta)$-$[Co(en)_2ox]PF_6$, which means that the two ethylenediamine rings of the cations

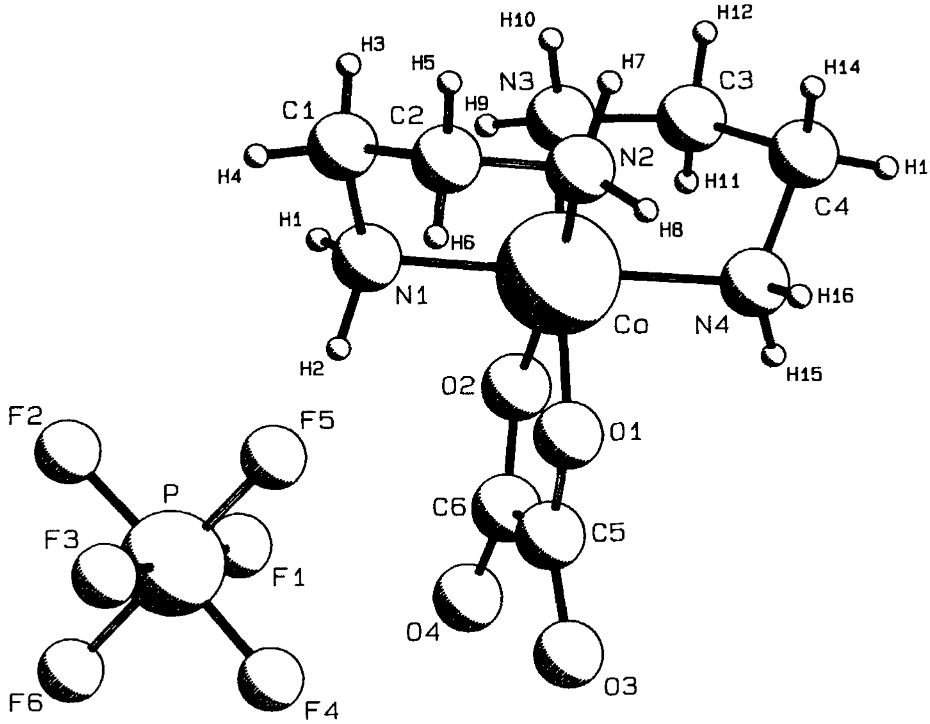

Figure 3 The contents of the asymmetric unit of compound (**III**) and the labelling system used in numbering the atoms present therein. The anion and the water of crystallization were placed at the crystallographic positions nearest to the cations insofar as hydrogen bonded interactions are concerned.

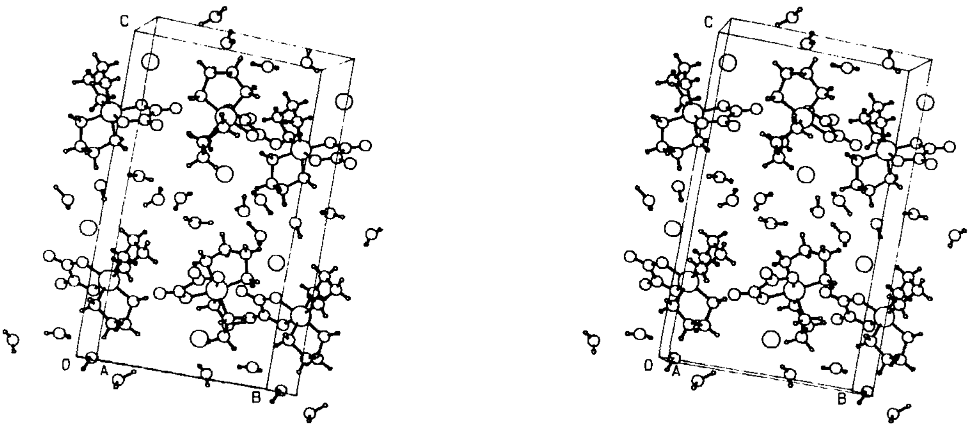

Figure 4 The contents of the unit cell of compound (**I**). This is a stereo pair. Note the spiral ribbons of cations running along the *b* axis and at heights of *ca* 1/4 and 3/4 in *c*. Also note the hydrogen bonded anions and waters holding the spirals together.

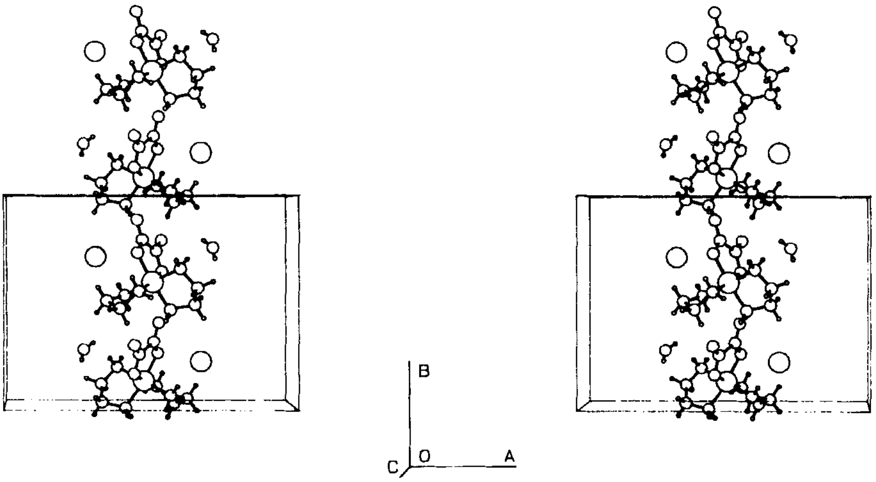

Figure 5 The contents of the unit cell of compound (II). This is a stereo pair. Note the spiral ribbons of cations running along the *b* axis and at heights of *ca* o, 1/2 and 1 in *c*. Also note the hydrogen bonded anions and waters holding the spirals together. Therefore, despite the difference in the number of the waters of hydration, and the sizes of the anions, the two compounds (I) and (II) have remarkably similar packing modes.

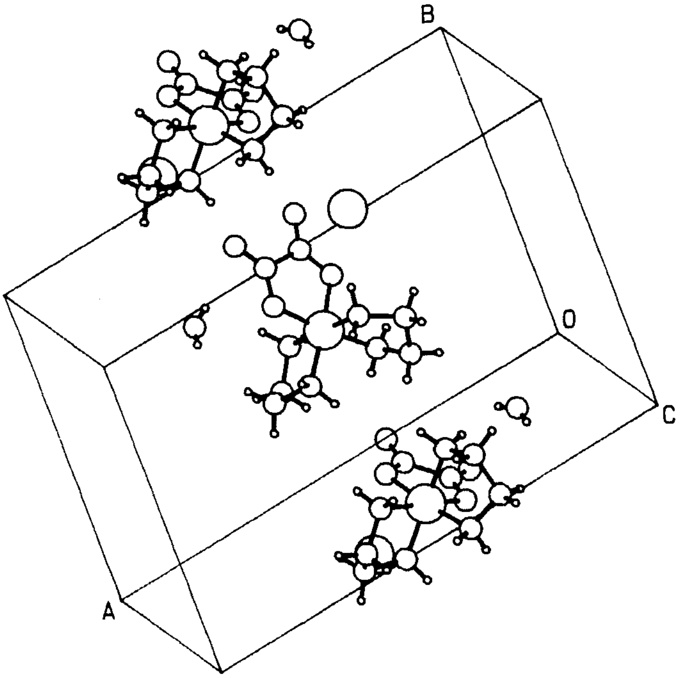

Figure 6 This view was drawn to illustrate as clearly as possible the interactions of the cations in both (I) and (II); consequently, only three cations belonging to a single spiral string, together with their anions and waters crystallization are shown. The model was derived from (II); however, the same results can be obtained using (I).

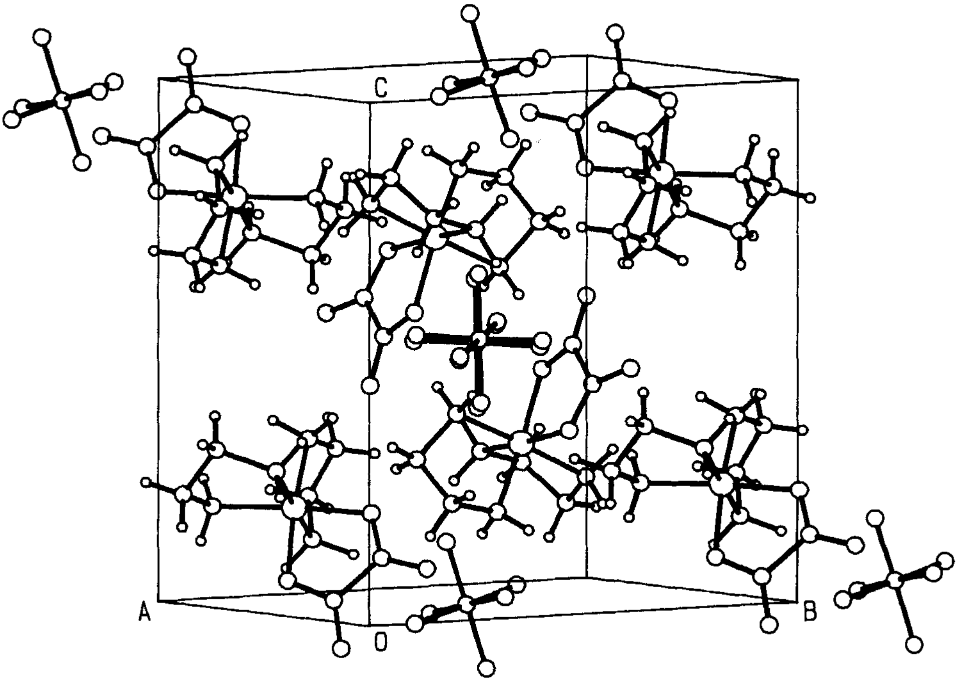

Figure 7 The contents of the unit cell of compound (III). Note the holes created by a group of four cations clustered about the inversion centre (1/2, 1/2, 1/2) and currently occupied by two anions. Other anions similarly fill the other holes shown; however, these were omitted for clarity.

of (I) and (II) are opposite in conformation, one λ(N1-C1-C2-N2) and one δ(N2-C3-C4-N4); both of those in (III) are δ. Therefore, in (I) and (II), the two ethylenediamines do not have the lowest possible conformational energies while in (III) they do. Such a confirmational feature has been previously observed[15] in the series $\Delta(\lambda\delta)$-[Co(en)$_2$(NO$_2$)$_2$]X (X = Cl, Br) and the phenomenon was then attributed to hydrogen bonded interactions. Clearly, the same is the case in (I) and (II) but not in (III), and we now explore the reasons why this may be so.

Reference to the tables of hydrogen bonds and to the packing diagrams reveal the interesting fact that there are short bonds between the oxalato cations in all three cases and despite the differences in waters of hydration in (I) and (II), the scheme of inter-cation hydrogen bonds is very much the same for these two compounds—terminal oxygen O3 of one oxalato cation forms a pair of bonds with hydrogens of both equatorial -NH$_2$ moieties (e.g., for (I), with H8 = 2.05Å, with with H10 = 2.06Å) in what could be described as a fairly rigid, bidentate fashion. At the same time, O4 forms a bond with an axial -NH$_2$ hydrogen (O4...H2 = 2.14Å) thus completing a sturdy three point attachment between adjacent cation pairs. In the case of (II), a similar pattern is noted (O3...H8 = 2.05Å and O3...H10 = 2.14Å; O4...H16 = 2.21Å). Such a classical, three-point chiral recognition pattern of hydrogen bonded attachments leads to the formation of spiral-shaped concatenated cations, every link of which is homochiral, and every spiral in the lattice is of the same chirality. In turn, anions and waters link these strings by inter-string hydrogen bonds. Figures 4 and 5 show

Table 5 Positional parameters and eds's for (I)

Atom	*x*/*a*	*y*/*b*	*z*/*c*	B(Å^2)
Co	0.3257(2)	0.06240(7)	0.23620(5)	1.38(1)
Cl	−0.1436(3)	−0.0415(2)	0.3877(1)	3.02(4)
O1	0.3274(8)	−0.0829(3)	0.2760(2)	1.66(9)
O2	0.0509(8)	0.0217(4)	0.2025(3)	1.9(1)
O3	0.1296(8)	−0.2364(4)	0.2791(3)	2.2(1)
O4	−0.1692(9)	−0.1242(4)	0.2064(3)	2.5(1)
N1	0.197(1)	0.1276(4)	0.3144(3)	1.8(1)
N2	0.5916(9)	0.0992(5)	0.2781(3)	1.8(1)
N3	0.315(1)	0.2024(4)	0.1888(3)	1.7(1)
N4	0.460(1)	0.0022(5)	0.1578(3)	1.7(1)
C1	0.358(1)	0.1431(6)	0.3667(4)	2.4(2)
C2	0.555(1)	0.1808(6)	0.3308(4)	2.4(2)
C3	0.349(1)	0.1797(6)	0.1178(4)	2.6(2)
C4	0.522(1)	0.0944(6)	0.1127(4)	2.6(2)
C5	0.163(1)	−0.1404(5)	0.2627(4)	1.6(1)
C6	−0.003(1)	−0.0776(5)	0.2208(4)	1.7(1)
Ow1	0.183(1)	−0.1206(5)	0.0581(3)	4.6(2)
Ow2	0.053(1)	−0.3326(6)	0.0149(4)	6.2(2)
Ow3	0.304(1)	0.1986(5)	−0.0478(3)	4.9(2)
Ow4	−0.024(1)	0.0811(6)	0.0040(3)	4.5(2)
Hw11	0.0566	−0.0605	0.0527	5*
Hw12	0.1113	−0.1777	0.0527	5
Hw21	0.1113	−0.3828	0.0351	5
Hw22	0.1093	−0.3242	−0.0175	5
Hw31	0.4433	0.1777	−0.0683	5
Hw32	0.3319	0.2656	−0.0156	5
Hw41	0.3885	0.4413	0.0351	5
Hw42	0.5546	0.4413	0.0000	5
H1	0.0893	0.0792	0.3301	5
H2	0.1373	0.1981	0.3034	5
H3	0.3834	0.0747	0.3891	5
H4	0.3142	0.1984	0.3972	5
H5	0.6713	0.1823	0.3600	5
H6	0.5338	0.2532	0.3126	5
H7	0.6522	0.0333	0.2961	5
H8	0.6849	0.1302	0.2464	5
H9	0.4216	0.2510	0.2046	5
H10	0.1806	0.2362	0.1948	5
H11	0.3899	0.2465	0.0959	5
H12	0.2237	0.1514	0.0985	5
H13	0.6528	0.1258	0.1259	5
H14	0.5331	0.0676	0.0687	5
H15	0.5827	−0.0385	0.1702	5
H16	0.3649	−0.0462	0.1357	5

*Hydrogen atoms of the Co cation were added at idealized positions (see text). Hydrogen atoms of the water of crystallization were found experimentally. All hydrogen atoms were assigned fixed thermal parameters of 5.00Å^2. Anisotropically refined atoms are given in the form of the isotropic equivalent thermal parameter defined as

$$(4/3)*[a^2*\beta_{11}+b^2*\beta_{22}+c^2*\beta_{33}+ab(\cos\gamma)*\beta_{12}+ac(\cos\beta)*\beta_{13}+bc(\cos\alpha)*\beta_{23}].$$

this effect clearly; specifically, in Figure 4, one can see the strings running along the *b*-axis and at heights of *ca* 1/4 and 3/4 in *c*. The same is true of Figure 5, where the strings run also along the *b*-axis and are located at *ca* 0, 1/2 and 1 in *c*. Halides and waters are located between the cationic strings and help hold them together, as can be ascertained by the hydrogen bonds listed in Tables 8 to 10.

Table 6 Positional parameters and eds's for (II)

Atom	x/a	y/b	z/c	$B(\text{Å}^2)$
Br	0.31585(5)	0.70669(6)	0.1008(1)	2.58(1)
Co	0.50925(6)	0.59207(6)	0.5714(1)	1.35(1)
Ow	0.7252(5)	0.7537(6)	0.412(1)	7.7(2)
O1	0.4576(3)	0.7305(3)	0.5837(8)	1.93(9)
O2	0.5475(3)	0.6367(3)	0.2892(7)	1.8(1)
O3	0.4586(3)	0.8869(3)	0.4019(8)	2.4(1)
O4	0.5491(3)	0.7851(3)	0.0812(7)	2.4(1)
N1	0.6031(4)	0.6546(4)	0.7131(8)	1.7(1)
N2	0.5725(4)	0.4593(4)	0.557(1)	1.8(1)
N3	0.4588(4)	0.5541(4)	0.8459(8)	1.8(1)
N4	0.4156(4)	0.5259(4)	0.435(1)	1.9(1)
C1	0.6604(5)	0.5689(5)	0.783(1)	2.5(2)
C2	0.6569(5)	0.4858(5)	0.600(1)	2.5(2)
C3	0.3951(5)	0.4715(5)	0.806(1)	2.3(2)
C4	0.3522(5)	0.5042(5)	0.599(1)	2.6(2)
C5	0.4764(4)	0.7910(4)	0.422(1)	1.5(1)
C6	0.5296(5)	0.7359(5)	0.245(1)	1.7(1)
Hw1	0.6914	0.7872	0.4122	5*
Hw2	0.7324	0.7012	0.4122	5
H1	0.5862	0.6944	0.8379	5
H2	0.6295	0.7017	0.6133	5
H3	0.6439	0.5379	0.9180	5
H4	0.7134	0.5973	0.7976	5
H5	0.6851	0.4225	0.6429	5
H6	0.6809	0.5148	0.4715	5
H7	0.5536	0.4096	0.6639	5
H8	0.5676	0.4281	0.4156	5
H9	0.4352	0.6167	0.9092	5
H10	0.4982	0.5255	0.9428	5
H11	0.3583	0.4699	0.9251	5
H12	0.4188	0.4022	0.7886	5
H13	0.3210	0.5674	0.6236	5
H14	0.3181	0.4474	0.5502	5
H15	0.3949	0.5733	0.3265	5
H16	0.4313	0.4598	0.3685	5

*Hydrogen atoms of cation were added at idealized positions (see text). Hydrogens of the water of crystallization were found experimentally. All hydrogen atoms were assigned fixed thermal parameters set at 5.0Å^2. Anisotropically refined atoms are given in the form of the isotropic equivalent thermal parameter defined as:

$$(4/3)*[a^2*\beta_{11}+b^2*\beta_{22}+c^2*\beta_{33}+ab(\cos\gamma)*\beta_{12}+ac(\cos\beta)*\beta_{13}+bc(\cos\alpha)*\beta_{23}].$$

In order to remove some of the clutter of Figures 4 and 5, and to simplify the illustration of the nature of the spiral strings wrapped around the two-fold screw axes, Figure 6 was drawn with a single string of hydrogen bonded cations together with their associated waters and halides (bromides). The left pair of cations shows the oxalato...H_2N- mode of hydrogen bonding most clearly.

The hydrogen bonding arrangement in (III) is different (see Figure 7) and we suspect the PF_6-anion is responsible for the change in hydrogen bonding mode, as can be appreciated from Figures 3 and 7 which shows that the anion is hydrogen bonded to H2 of N1 (*via* both F1 and F5) and is so positioned as to pre-empt chances of a bidentate hydrogen bonding mode for the oxalate. Note that F1 and F4 block access to O4, which then has relatively long hydrogen bonds. The resulting hydrogen bonding

Table 7 Positional parameters and eds's for (III)

Atom	x/a	y/b	z/c	$B(\text{Å}^2)$
Co	0.4696(2)	0.9141(1)	0.8018(1)	1.38(3)
P	0.9771(5)	0.7611(3)	0.9705(3)	2.86(9)
F1	0.812(1)	0.8011(8)	1.0128(8)	4.9(3)
F2	1.040(1)	0.8783(8)	0.980(1)	8.3(4)
F3	1.141(1)	0.7251(8)	0.9274(9)	5.6(3)
F4	0.919(1)	0.6427(8)	0.965(1)	6.6(3)
F5	0.925(1)	0.783(1)	0.8530(9)	8.5(4)
F6	1.026(1)	0.739(1)	1.0905(8)	6.5(3)
O1	0.540(1)	0.7686(7)	0.8168(7)	2.2(2)
O2	0.405(1)	0.8977(7)	0.9461(7)	2.2(2)
O3	0.525(1)	0.6313(7)	0.9296(7)	2.2(2)
O4	0.427(1)	0.7832(7)	1.0790(7)	2.5(2)
N1	0.665(1)	0.9682(9)	0.8517(9)	3.7(3)
N2	0.560(1)	0.9255(9)	0.6654(9)	4.1(3)
N3	0.373(1)	1.0573(8)	0.7977(8)	3.3(3)
N4	0.274(1)	0.8594(9)	0.7442(9)	3.7(3)
C1	0.750(2)	1.020(1)	0.763(1)	3.9(4)
C2	0.731(2)	0.947(1)	0.675(1)	3.1(4)
C3	0.205(2)	1.043(1)	0.784(1)	3.6(4)
C4	0.180(2)	0.953(1)	0.702(1)	3.3(4)
C5	0.509(1)	0.729(1)	0.906(1)	1.7(3)
C6	0.443(2)	0.807(1)	0.986(1)	2.9(3)
H1	0.6485	1.0204	0.9055	5*
H2	0.7241	0.9098	0.8794	5
H3	0.7074	1.0886	0.7467	5
H4	0.8556	1.0273	0.7803	5
H5	0.7683	0.9798	0.6118	5
H6	0.7852	0.8811	0.6870	5
H7	0.5123	0.9835	0.6280	5
H8	0.5434	0.8596	0.6280	5
H9	0.3928	1.0945	0.8618	5
H10	0.4128	1.0979	0.7404	5
H11	0.1597	1.0225	0.8488	5
H12	0.1598	1.1081	0.7590	5
H13	0.0742	0.9336	0.6978	5
H14	0.2151	0.9746	0.6349	5
H15	0.2188	0.8234	0.7983	5
H16	0.2943	0.8098	0.6886	5

*Hydrogen atoms were added at idealized positions with fixed thermal parameters of 5.0Å^2. Anisotropically refined atoms are given in the form of the isotropic equivalent thermal parameter defined as:

$$(4)3/*[a^2*\beta_{11}+b^2*\beta_{22}+c^2*\beta_{33}+ab(\cos\gamma)*\beta_{12}+ac(\cos\beta)*\beta_{13}+bc(\cos\alpha)*\beta_{23}].$$

scheme changes in the following ways: (a) the interactions between cations are not between terminal O3 and O4 of one cation to the basal plane and axial -NH_2 hydrogens of a second one; (b) instead, both oxygens of a given oxalato carbon (one terminal and one bonded to cobalt) link a pair of axial and equatorial -NH_2 hydrogens; (c) this arrangement gives rise to a ring of four cations disposed around the inversion centre at 1/2, 1/2, 1/2, as shown in Figure 7; (d) since the PF_6-anion is able to equally well form hydrogen bonds with fluorines located on either side, it is not surprising to note that the P atom is located at a *pseudo*-inversion centre of the lattice at *ca* 0, 3/4, 0 (see Table 9). This feature can readily be observed in Figure 7; (e) finally, note

Table 8 Bond distances (Å) and angles (°) for (I)

A) Distances

Atom 1	Atom 2	Distance	Atom 1	Atom 2	Distance
Co	O1	1.916(2)	N4	C4	1.485(5)
Co	O2	1.935(3)	C1	C2	1.511(6)
Co	N1	1.949(4)	C3	C4	1.500(6)
Co	N2	1.939(3)	C5	C6	1.547(6)
Co	N3	1.932(3)	Ow1	Hw11	1.082(4)
Co	N4	1.946(4)	Ow1	Hw12	0.827(4)
O1	C5	1.279(5)	Ow2	Hw21	0.817(4)
O2	C6	1.290(4)	Ow2	Hw22	0.756(5)
O3	C5	1.213(4)	Ow3	Hw31	1.006(4)
O4	C6	1.228(5)	Ow3	Hw32	1.050(3)
N1	C1	1.487(6)	Ow4	Hw41	1.006(4)
N2	C2	1.467(5)	Ow4	Hw42	0.571(4)
N3	C3	1.484(6)			

B) Angles

Atom 1	Atom 2	Atom 3	Angle	Atom 1	Atom 2	Atom 3	Angle
O1	Co	O2	85.8(1)	N3	C3	C4	107.5(4)
O1	Co	N1	91.2(1)	N4	C4	C3	105.7(4)
O1	Co	N2	90.9(1)	O1	C5	O3	126.3(4)
O1	Co	N3	174.8(1)	O1	C5	C6	114.2(3)
O1	Co	N4	90.5(1)	O3	C5	C6	119.5(4)
O2	Co	N1	90.7(2)	O2	C6	O4	125.1(4)
O2	Co	N2	174.6(2)	O2	C6	C5	115.2(3)
O2	Co	N3	90.6(1)	O4	C6	C5	119.6(3)
O2	Co	N4	90.7(1)	Hw11	Ow1	Hw12	97.4(4)
N1	Co	N2	85.2(2)	Hw21	Ow2	Hw22	108.6(6)
N1	Co	N3	92.5(1)	Hw31	Ow3	Hw32	107.4(4)
N1	Co	N4	177.9(1)	Hw41	Ow4	Hw42	104.0(5)
N2	Co	N3	93.0(2)				
N2	Co	N4	93.5(2)				
N3	Co	N4	85.9(1)				
Co	O1	C5	113.2(3)				
Co	O2	C6	111.6(3)				
Co	N1	C1	110.1(3)				
Co	N2	C2	109.4(3)				
Co	N3	C3	108.7(2)				
Co	N4	C4	110.2(3)				
N1	C1	C2	105.1(3)				
N2	C2	C1	106.6(3)				

C) Torsion Angles

Atom 1	Atom 2	Atom 3	Atom 4	Angle	Atom 1	Atom 2	Atom 3	Atom 4	Angle
O2	Co	O1	C5	1.7	N1	Co	N3	C3	−164.8
N1	Co	O1	C5	92.3	N2	Co	N3	C3	109.9
N2	Co	O1	C5	177.5	N4	Co	N3	C3	16.6
N3	Co	O1	C5	−43.6	O1	Co	N4	C4	−171.9
N4	Co	O1	C5	−89.0	O2	Co	N4	C4	102.4
O1	Co	O2	C6	0.1	N1	Co	N4	C4	−29.9
N1	Co	O2	C6	−91.1	N2	Co	N4	C4	−80.9
N2	Co	O2	C6	−51.7	N3	Co	N4	C4	11.9
N3	Co	O2	C6	176.4	Co	O1	C5	O3	176.2
N4	Co	O2	C6	90.5	Co	O1	C5	C6	−2.9
O1	Co	N1	C1	77.7	Co	O2	C6	O4	−180.0

Table 8 Bond distances (Å) and angles (°) for (I) *continued*

C) Torsion Angles

Atom 1	Atom 2	Atom 3	Atom 4	Angle	Atom 1	Atom 2	Atom 3	Atom 4	Angle
O2	Co	N1	C1	163.5	Co	O2	C6	C5	−1.5
N2	Co	N1	C1	−13.1	Co	N1	C1	C2	38.7
N3	Co	N1	C1	−105.9	Co	N2	C2	C1	42.5
N4	Co	N1	C1	−64.2	Co	N3	C3	C4	−41.5
O1	Co	N2	C2	−108.0	Co	N4	C4	C3	−36.9
O2	Co	N2	C2	−56.4	N1	C1	C2	N2	−52.2
N1	Co	N2	C2	−16.8	N3	C3	C4	N4	50.6
N3	Co	N2	C2	75.5	O1	C5	C6	O2	3.0
N4	Co	N2	C2	161.5	O1	C5	C6	O4	−178.4
O1	Co	N3	C3	−29.0	O3	C5	C6	O2	−176.1
O2	Co	N3	C3	−74.1	O3	C5	C6	O4	2.4

D) Selected List of Hydrogen Bonds

Cl-H1	2.374	N1-H1...Cl	169.5	
Ow1-H16	2.148	N4-H16...Ow1	160.2	
Ow2-Hw12	2.039	Ow1-Hw12...Ow2	154.1	
Ow4-Hw11	2.026	Ow1-Hw11...Ow4	142.3	
Cl-Hw21	2.471	Ow2-Hw21...Cl	157.2	Ow2 at $-x$, $1/2+y$, $1/2-z$
Cl-Hw31	2.250	Ow3-Hw31...Cl	146.9	Ow3 at $1/2+x$, $1/2-y$, $-z$
Cl-Hw41	2.217	Ow4-Hw41...Cl	166.0	Ow4 at $-x$, $-1/2+y$, $1/2-z$
Cl-H7	2.436	N2-H7...Cl	144.6	N2 at $-1+x$, y, z
O3-H8	2.048	N2-H8...O3	146.5	N2 at $1-x$, $-1/2+y$, $1/2-z$
O3-H10	2.064	N3-H10...O3	162.7	N3 at $-x$, $-1/2+y$, $1/2-z$
O4-H2	2.144	N1-H2...O4	149.7	N1 at $-x$, $-1/2+y$, $1/2-z$
O4-H15	2.016	N4-H15...O4	174.0	N4 at $-1+x$, y, z
Ow3-Hw42	2.500	Ow4-Hw42...Ow3	107.0	Ow4 at $-1/2+x$, $1/2-y$, $-z$
Ow4-Hw32	2.062	Ow3-Hw32...Ow4	145.5	Ow3 at $-1/2+x$, $1/2-y$, $-z$

Table 9 Bond distances (Å) and angles (°) for (II)

A) Distances

Atom 1	Atom 2	Distance
Co	O1	1.917(2)
Co	O2	1.918(2)
Co	N1	1.942(3)
Co	N2	1.951(3)
Co	N3	1.932(3)
Co	N4	1.944(3)
Ow	Hw1	0.697(4)
Ow	Hw2	0.661(4)
O1	C5	1.277(4)
O2	C6	1.291(4)
O3	C5	1.229(3)
O4	C6	1.217(4)
N1	C1	1.486(4)
N2	C2	1.459(5)
N3	C3	1.489(5)
N4	C4	1.477(5)
C1	C2	1.521(5)
C3	C4	1.511(6)
C5	C6	1.554(5)

Table 9 Bond distances (Å) and angles (°) for (II) *continued*

B) Angles

Atom 1	Atom 2	Atom 3	Angle	Atom 1	Atom 2	Atom 3	Angle
O1	Co	O2	85.7(1)	Co	N1	C1	110.8(2)
O1	Co	N1	89.1(1)	Co	N2	C2	108.6(2)
O1	Co	N2	174.0(1)	Co	N3	C3	109.5(2)
O1	Co	N3	89.4(1)	Co	N4	C4	110.7(3)
O1	Co	N4	92.1(1)	N1	C1	C2	104.3(3)
O2	Co	N1	91.2(1)	N2	C2	C1	108.6(3)
O2	Co	N2	91.4(1)	N3	C3	C4	106.6(3)
O2	Co	N3	173.3(1)	N4	C4	C3	106.5(3)
O2	Co	N4	89.9(1)	O1	C5	O3	125.9(3)
N1	Co	N2	85.6(1)	O1	C5	C6	114.7(3)
N1	Co	N3	93.3(1)	O3	C5	C6	119.4(3)
N1	Co	N4	178.4(1)	O2	C6	O4	126.0(3)
N2	Co	N3	93.8(1)	O2	C6	C5	113.8(3)
N2	Co	N4	93.2(1)	O4	C6	C5	120.2(3)
N3	Co	N4	85.7(1)	Hw1	Ow	Hw2	136.8(6)
Co	O1	O3	138.8(2)				
Co	O1	C5	112.7(2)				
O3	O1	C5	26.5(2)				
Co	O2	O4	138.7(1)				
Co	O2	C6	112.6(2)				
O4	O2	C6	26.2(2)				
O1	O3	C5	27.6(2)				
O2	O4	C6	27.9(2)				

C) Torsion angles

Atom 1	Atom 2	Atom 3	Atom 4	Angle	Atom 1	Atom 2	Atom 3	Atom 4	Angle
O2	Co	O1	C5	−6.2	O1	C5	C6	O2	−0.4
N1	Co	O1	C5	85.1	O1	C5	C6	O4	177.8
N2	Co	O1	C5	55.7	O3	C5	C6	O2	176.9
N3	Co	O1	C5	178.4	O3	C5	C6	O4	−4.8
N4	Co	O1	C5	−95.9					
O1	Co	O2	C6	5.9					
N1	Co	O2	C6	−83.1					
N2	Co	O2	C6	−168.8					
N3	Co	O2	C6	49.2					
N4	Co	O2	C6	98.0					
O1	Co	N1	C1	169.1					
O2	Co	N1	C1	−105.2					
N2	Co	N1	C1	−13.9					
N3	Co	N1	C1	79.7					
N4	Co	N1	C1	30.0					
O1	Co	N2	C2	14.5					
O2	Co	N2	C2	76.0					
N1	Co	N2	C2	−15.1					
N3	Co	N2	C2	−108.1					
N4	Co	N2	C2	166.0					
O1	Co	N3	C3	109.0					
O2	Co	N3	C3	65.8					
N1	Co	N3	C3	−161.9					
N2	Co	N3	C3	−76.1					
N4	Co	N3	C3	16.9					

Table 9 Bond distances (Å) and angles (°) for (II) *continued*

C) Torsion angles

Atom 1	Atom 2	Atom 3	Atom 4	Angle	Atom 1	Atom 2	Atom 3	Atom 4	Angle
O1	Co	N4	C4	−78.0					
O2	Co	N4	C4	−163.7					
N1	Co	N4	C4	61.1					
N2	Co	N4	C4	104.9					
N3	Co	N4	C4	11.3					
Co	O1	C5	O3	−172.0					
Co	O1	C5	C6	5.2					
Co	O2	C6	O4	177.3					
Co	O2	C6	C5	−4.5					
Co	N1	C1	C2	37.8					
Co	N2	C2	C1	40.5					
Co	N3	C3	C4	−40.6					
Co	N4	C4	C3	−36.1					
N1	C1	C2	N2	−50.7					
N3	C3	C4	N4	49.2					

D) Selected List of Hydrogen Bonds

Br-H15	2.518	N4-H15...Br	167.3	
Ow-H2	2.109	N1-H2...Ow	155.3	
Br-H9	2.555	N3-H9...Br	149.5	N3 at *x*, *y*, −1+*z*
O3-H8	2.052	N2-H8...O3	168.2	N2 at 1−*x*, 1/2+*y*, 1/2−*z*
O3-H10	2.087	N3-H10...O3	145.7	N3 at 1−*x*, 1/2+*y*, 1.5−*z*
O4-H1	1.962	N1-H1...O4	175.8	N1 at *x*, *y*, −1+*z*
O4-H16	2.207	N4-H16...O4	145.5	N4 at 1−*x*, 1/2+*y*, 1/2−*z*

Table 10 Bond distances (Å) and angles (°) for (III)

A) Distances

Atom 1	Atom 2	Distance	Atom 1	Atom 2	Distance
Co	O1	1.904(3)	P	F1	1.611(4)
Co	O2	1.927(3)	P	F2	1.549(4)
Co	N1	1.930(5)	P	F3	1.592(4)
Co	N2	1.908(5)	P	F4	1.547(4)
Co	N3	1.956(4)	P	F5	1.578(4)
Co	N4	1.966(5)	P	F6	1.600(4)
O1	C5	1.258(6)			
O2	C6	1.265(6)			
O3	C5	1.253(6)			
O4	C6	1.223(6)			
N1	C1	1.492(7)			
N2	C2	1.521(7)			
N3	C3	1.482(7)			
N4	C4	1.508(7)			
C1	C2	1.441(8)			
C3	C4	1.526(8)			
C5	C6	1.518(7)			

Table 10 Bond distances (Å) and angles (°) for (III) *continued*

B) Angles

Atom 1	Atom 2	Atom 3	Angle
O1	Co	O2	84.3(2)
O1	Co	N1	90.7(2)
O1	Co	N2	91.5(2)
O1	Co	N3	172.1(2)
O1	Co	N4	89.4(2)
O2	Co	N1	89.2(2)
O2	Co	N2	172.5(2)
O2	Co	N3	89.6(2)
O2	Co	N4	93.5(2)
N1	Co	N2	84.6(2)
N1	Co	N3	94.3(2)
N1	Co	N4	177.3(2)
N2	Co	N3	95.0(2)
N2	Co	N4	92.7(2)
N3	Co	N4	85.9(2)
F1	P	F2	90.0(2)
F1	P	F3	178.3(2)
F1	P	F4	90.7(2)
F1	P	F5	90.6(2)
F1	P	F6	88.1(2)
F2	P	F3	88.4(2)
F2	P	F4	177.6(4)
F2	P	F5	90.7(3)
F2	P	F6	89.4(3)
F3	P	F4	90.9(2)
F3	P	F5	88.6(3)
F3	P	F6	92.6(2)
F4	P	F5	91.6(3)
F4	P	F6	88.3(3)
F5	P	F6	178.8(3)
Co	O1	C5	112.5(3)
Co	O2	C6	113.4(4)
Co	N1	C1	109.7(4)
Co	N2	C2	110.6(4)
Co	N3	C3	108.5(3)
Co	N4	C4	109.6(3)
N1	C1	C2	105.6(5)
N2	C2	C1	105.9(5)
N3	C3	C4	107.8(5)
N4	C4	C3	104.0(4)
O1	C5	O3	124.3(5)
O1	C5	C6	116.1(5)
O3	C5	C6	119.6(5)
O2	C6	O4	124.8(5)
O2	C6	C5	112.8(5)
O4	C6	C5	122.4(5)

C) Torsional Angles

Atom 1	Atom 2	Atom 3	Atom 4	Angle	Atom 1	Atom 2	Atom 3	Atom 4	Angle
O2	Co	O1	C5	2.6	N1	Co	N3	C3	−167.7
N1	Co	O1	C5	91.7	N2	Co	N3	C3	107.3
N2	Co	O1	C5	176.4	N4	Co	N3	C3	15.0
N3	Co	O1	C5	−37.7	O1	Co	N4	C4	−171.4
N4	Co	O1	C5	−91.0	O2	Co	N4	C4	104.3

Table 10 Bond distances (Å) and angles (°) for (III) *continued*

C) Torsional Angles

Atom 1	Atom 2	Atom 3	Atom 4	Angle	Atom 1	Atom 2	Atom 3	Atom 4	Angle
O1	Co	O2	C6	3.8	N1	Co	N4	C4	−79.5
N1	Co	O2	C6	−87.0	N2	Co	N4	C4	−79.9
N2	Co	O2	C6	−53.0	N3	Co	N4	C4	15.0
N3	Co	O2	C6	178.6	Co	O1	C5	O3	170.7
N4	Co	O2	C6	92.8	Co	O1	C5	C6	−7.6
O1	Co	N1	C1	109.3	Co	O2	C6	O4	172.7
O2	Co	N1	C1	−166.3	Co	O2	C6	C5	−8.2
N2	Co	N1	C1	17.8	Co	N1	C1	C2	−43.8
N3	Co	N1	C1	−76.8	Co	N2	C2	C1	−38.0
N4	Co	N1	C1	17.5	Co	N3	C3	C4	−41.7
O1	Co	N2	C2	−79.8	Co	N4	C4	C3	−40.0
O2	Co	N2	C2	−23.4	N1	C1	C2	N2	51.3
N1	Co	N2	C2	10.8	N3	C3	C4	N4	52.9
N3	Co	N2	C2	104.7	O1	C5	C6	O2	10.9
N4	Co	N2	C2	−169.2	O1	C5	C6	O4	−170.1
O1	Co	N3	C3	−38.5	O3	C5	C6	O2	−167.5
O2	Co	N3	C3	−78.5	O3	C5	C6	O4	11.6

D) Selected List of Hydrogen Bonds

F1-H2	2.286	N1-H2...F1	153.6	
F5-H2	2.369	N1-H2...F5	147.6	
F3-H15	2.150	N4-H15...F3	167.5	N4 at $1+x$, y, z
O1-H10	2.264	N3-H10...O1	143.5	N3 at $1-x$, $-1/2+y$, $1.5-z$
O3-H7	1.990	N2-H7...O3	160.5	N2 at $1-x$, $-1/2+y$, $1.5-z$
O3-H10	2.263	N3-H10...O3	156.1	N3 at $1-x$, $-1/2+y$, $1.5-z$
O4-H8	2.123	N2-H8...O4	157.5	N2 at x, $1\text{-}5-y$, $1/2+z$
O4-H16	2.145	N4-H16...O4	158.1	N4 at x, $1.5-y$, $1/2+z$

that the PF_6-anion is located in channels formed by the cations (Figure 7) and hydrogen bonding ability and bulk is sufficient to prevent the cations from interacting in the same fashion as they do in (**I**) and (**II**).

We now come to the iodide derivative (**IV**). Unfortunately we could not obtain a good structure from the homochiral crystals (space group $C2$, $Z=2$, see Table 4). The heterochiral crystals (space group, apparently, $C2/c$) are even of lesser quality. Interestingly, and consistent with our difficulties with crystals of (**IV**), Marusak *et al.*[16] have determined the structure of $[Co(N,N'\text{-}Me_2en)_2ox]I{\cdot}2H_2O$, which they report as forming extremely fragile crystals, highly susceptible to mechanical fracture and unstable under X-ray irrradiation. Our crystals of both iodide forms have highly variable peak shapes and widths, suggesting they are equally affected by mechanical instability, which may be associated with the forcing of the cationic lattice apart by the bulky iodide anions, despite having squeezed out the waters of crystallization. The I anion and the Co(oxalate) fragment of the $C2$ form were found to lie at a two-fold axis without disorder of the fragment. However, the two ethylenediamine ligands were badly disordered, and difference maps suggested two or more sites for atoms in the approximate positions expected for these ligands and separated by small distances of *ca* 0.2 to 0.3Å. These difference maps suggest the disorder is due to the opposite chirality of en rings, as was the case with (I) and (II). This is a reasonable speculation which would justify the disorder while answering two questions as to why, unlike the chloride and the bromide, the iodide is capable of crystallizing as a conglomerate and as a racemate and why does the degree of hydration decrease with the size of the counterranion, as observed. A reasonable answer to the former is that if the bulk of the iodide is such that it interferes with the hydrogen bonding of the cations, the difference in packing energy in the two crystalline forms may be very small, which may also account for the poor quality of the crystals. We note here that the refinement of (III) is the poorest in quality, while that of (I) and (II) are approximately the same despite the fact that some data were lost in the former case. In fact, either refinement is markedly superior to that of (III). The answer to the second is that, irrespective of the nature of the intercationic hydrogen bonding network, the anions and waters (if any) are located in channels created by the cationic network. If this network is to be preserved as strongly as possible, the effective volume available to pack anions and waters is limited. Note that (I) and (II) crystallize in the same space group and that one may imagine the bromide anion squeezing some of the water out of the channels in order to fit in the cationic framework. If this is a reasonable explanation, the iodide would, then, be expected to squeeze out the last water of crystallization present in the bromide.

Finally, we come to the heterochiral iodide crystals (assumed to be $C2/c$ from indexing, systematic absences showing the c-glide and the similarity to the cell given by Bigoli *et al.*[17] for the closely related compound, $[Co(en)_2CO_3]I{\cdot}2H_2O$). If this latter assumption is correct, the crystals would have disordered cations since, given the unit cell volume, and a reasonable density of *ca* 2.2 (as was the case with the crystals in space group $C2$), z must be 4. This would place the cations and anions, once more, on a two fold axis, or even worse, at an inversion centre. We did not feel that the crystal quality warranted any further work on these specimens.

No effort was made to check the CD spectra of these crystals since none were large enough to carry out such measurements and, since both enantiomorphs are deposited during conglomerate crystallization, a negative result would be meaningless. Therefore, efforts at characterizing the iodide crystals beyond that provided by the work of Yamanari *et al.*[4] have been disappointing.

CONCLUSIONS

We feel that the conglomerate crystallization of (I) and (II) is caused by the formation of spiral strings of cations held together by strong $O...H_2N$- hydrogen bonds in which a terminal oxalato oxygen binds, in a bidentate fashion, a pair of basal plane hydrogens of an adjacent cation, while the second terminal oxygen binds a third hydrogen, located on an axial-NH_2, giving rise to a three-point chiral recognition pattern. Since the process can be repeated indefinitely, these spiral strings are a polymer extending as a single strand along the b-axis. Scale models show these hydrogen bonds are more effective when adjacent cations are twisted with respect to one another so as to expose the hydrogens to the non-bonded pairs of the terminal oxygens on oxalate, the formation of the first pair begins the spiral twist. Moreover, we know that these interactions persist in solution since deuterium exchange for the equatorial -NH_2 hydrogens of these oxalates is very slow, suggesting steric hindrance to access by D_2O molecules.[18]

In a racemic solution both types of spirals are formed, left handed and right handed, since the cations of a racemate are present equally as Λ and Δ. Thus, both types of spirals must form; however since they crystallize as homochiral crystals, the obvious conclusion is that the stitching together of the spirals, by the anions and the waters, must lead to better free energies of crystallization when they segregate into enantiomorphic lattices. Therefore, the observation by Yamanari *et al.*[4] that the iodide crystallizes in both classes of crystals, suggests that the iodide does not care whether it stitches homochiral or heterochiral strings, and this may be the origin of the disorder we have noted. Finally, the PF_6-anion must interfere in solution with the formation of strings similar to those formed by the halides since the packing we observe belongs to a totally different mode of cationic hydrogen bonding. Thus, control of crystallization mode seems to be associated with ion pair formation in solution which, in turn, determines the nature of the crystalline lattice selected.

In our experience with the *cis*-dinitro series (be it in $[Co(en)_2(NO_2)_2)X$ or $[Co(trien)_2(NO_2)_2)X$; X = Cl, Br, I), with $K[Co(edda)(NO_2)_2]$ (edda = ethylenediaminediacetic acid),[19] with $(Cat)[Co(etda)]\cdot 2H_2O$ (Cat = $NH4^+$, K^+, Rb^+)[20] and with the current series, the same pattern mentioned above is obeyed. Thus, we conclude that for conglomerate crystallization of these compounds there are three required ingredients.

1. **Rigidity of molecules** (ions) needs to be achieved, if not already there. Both the *cis*-dinitro series, the *cis*-α-$[Co(trien)(NO_2)_2]X\cdot H_2O$ (X = Cl,[15] I[22]) and *cis*-$[Co(en)_2(NO_2)_2]X$ (X = Cl,[15] Br,[21] I[21]), achieve this by strong intramolecular hydrogen bonds between -NO_2 oxygens and **axial** -NH_2 hydrogens. We have shown that if these hydrogen bonds are interfered with, racemate (heterochiral) crystals are obtained.[23] A simple way of causing such interference is the use of powerful hydrogen bonding anions such as NO_2- and NO_3-, both of which cause *cis*-$[Co(en)_2(NO_2)_2]X$ (X = NO_2- and NO_3-) to crystallize as racemates.[23] The current compound (**I**), as well as all those amine carboxylates listed in the Introduction, are rigid enough so that intramolecular interactions are probably a minor factor in the selection of a crystallization pathway. The same comments apply to the members of the series $[Co(en)_2oxalato]X\cdot nH_2O$ (X = Cl, n = 4; Br, n = 1 and I, n = 0) that crystallize as conglomerates and are rigid enough as such.[22]
2. **String formation in solution and in the solid state** seems to be an essential ingredient for all compounds thus far mentioned to crystallize as conglomerates and, if interfered with, results in racemates. We demonstrated this very clearly by comparison of the crystallization behavior of the three series *cis*-α-$[Co(trien)(NO_2)_2]X\cdot H_2O$ (X = Cl,[15] I[22]), *cis*-$[Co(en)_2(NO_2)_2]X$ (X = Cl,[15] Br,[21] I[21]) and $[Co(en)_2oxalato]X\cdot nH_2O$ (X = Cl, n = 4; Br, n = 1; I, n = 0),[21] all of which crystallize with polymeric, infinite spiral strings. Also, in order to test the importance of this phenomenon on crystallization pathway, we prepared the series $[Co(tn)_2oxalato]X\cdot H_2O$ (tn = 1,3-diaminopropane, X = Cl, Br, I) which we knew, from models, to be incapable of forming the spiral strings due to steric hindrance at the site of the necessary hydrogen bonds. Such an expectation was found to be correct, since, unlike their *bis*-ethylenediamine counterparts, the compounds of the series $[Co(tn)_2oxalato]X$ crystallize as racemates.[21] We know that association takes place in solution since, as mentioned above, deuterium exchange in the oxalato series is retarded,[18] suggesting that the associated ions slow down exchange of amine hydrogens due to hydrogen bonded interactions in fluid media.

3. **Interactions between strings** can be of two types: (a) direct interactions between strings, as in the two halves of a zipper, or protein strands, examples of which are found in the structures of *mer*-[$Co(NH_3)_3(NO_2)_3$] (space group $P2_12_12_1$)[25] and of *fac*-[$Co(NH_3)_3(NO_2)_3$] (space group $P2_12_12_1$);[26] (b) counter ions (and/or waters of crystallization, where relevant) are present, as is the case of (**I**) and of the diamine-*N*,*N*′-tetracarboxylates discussed above. In such cases, the strings are joined by the agency of the cations (and/or the waters of crystallization). In both cases, linkages must have a clear preference for joining strings of the same chirality; if not, either heterochiral crystals are obtained, or one obtains both conglomerates and racemates. An example of clear preference for heterochiral string formation is the case of [$Co(en)_2ox$]PF_6 which crystallizes as a racemate, unlike the chloride and bromide which crystallize as conglomerates.[21] An example of an ambiguous crystallization behaviour is [$Co(en)_2ox$]I, which crystallizes as both a racemate and a conglomerate. This latter result has been proven by phase diagram studies of the system.[4] We have preliminary crystallographic data on this iodide system; however, it is highly preliminary due to poor crystal quality. However, so far, our results[21] are in accord with those of Yamanari *et al.*[4]

Acknowledgements

We thank the Robert A. Welch Foundation for support of this research (Grant E-592 to I. Bernal) and for fellowships granted to J. Cetrullo and J. Myrczek. We thank the National Science Foundation for the funds used in purchasing the diffractometer.

Supplementary Material

Compound (**I**): anisotropic thermal parameters (1 page), structure factor table (9 pages). Compound (**II**): anisotropic thermal parameters (1 page), structure factor table (16 pages). Compound (**III**): anisotropic thermal parameters (1 page), structure factor table (9 pages). All are available from the authors upon request.

References

1. I. Bernal and J. Cetrullo, *Struct. Chem.*, **1**, 235 (1990).
2. A. Werner, *Chem. Ber.*, **47**, 2171 (1914).
3. K. Yamasaki, H. Igarishi and Y. Yoshikawa, *Inorg. Nuclear Chem. Letters*, **4**, 491 (1968).
4. K. Yamanari, J. Hidaka and Y. Shimura, *Bull. Chem. Soc. Japan*, **46**, 3724 (1973). Also, see A. Fuyuhiro, K. Yamanari and Y. Shimura, *Bull. Chem. Soc. Japan*, **54**, 2531 (1981).
5. R.D. Gillard and L.H.R. Tipping, *J. Chem. Soc., Dalton Trans.*, 1241 (1977).
6. T. Aoki, K. Matsumoto, S. Ooi and Y. Koroya, *Bull. Chem. Soc. Japan*, **46**, 159 (1973).
7. M.C. Couldwell, D.A. House and B.R. Penfold, *Inorg. Chim. Acta*, **13**, 13 (1975).
8. F.M. Jaeger and W. Thomas, *Proc. Acad. Sci. Amsterdam*, **22**, 693 (1919).
9. A.E.H. Tutton, "Crystallography and Practical Crystal Measurements", Second Edition, (Indian Printing Works, New Dehli, 1965); reprinted from the original (Macmillan, London, 1922), version. See Vol. 2, pp. 1282–1283.
10. J.C. Bailar, Jr., *Inorg. Syntheses*, **2**, 222 (1946).
11. TEXRAY-230 is a modification of the SDP-Plus[12] set of X-ray crystallographic programs distributed by the Molecular Structure Corporation, 3200 Research Forest Dr., The Woodlands, TX 77386, for use with their automation of the CAD-4 diffractometer.

12. SDP-Plus is the Enraf-Nonius Corporation X-ray diffraction data processing programs distributed by B.A. Frenz and Associates, 1140 East Harvey Road, College Station, TX, 77840.
13. R.B. Roof, "A Theoretical Extension of the Reduced Cell Concept in Crustallography", Report LA-4038, Los Alamos Scientific Laboratory (1969).
14. D.T. Cromer and J.T. Waber, "International Tables for X-Ray Crystallography", (Kynoch Press, Birmingham, England, 1975); Vol. IV, Tables 2.2.8 and 2.3.1, respectively, for the scattering factor curves and the anomalous dispersion values.
15. I. Bernal, *Inorg. Chim. Acta*, **96**, 99 (1985).
16. R.A. Marusak, M.A. Ivanca, K.J. Haller and A.G. Lappin, *Inorg. Chem.*, **30**, 618 (1991).
17. F. Bigoli, M. Lafranchi, E. Leporati and M.A. Pellinghelli, *Cryst. Struc. Commun.*, **9**, 1261 (1980).
18. (a) U. Sakaguichi, K. Maeda and H. Yoneda, *Bull. Chem. Soc. Japan*, **49**, 397 (1976); (b) U. Sakaguichi, S. Yamazaki and H. Yoneda, *Bull. Chem. Soc. Japan*, **49**, 402 (1976).
19. I. Bernal, J. Cetrullo, J. Myrczek and W.T. Jordan, unpublished results.
20. H.A. Weakliem and J.L. Hoard, *J. Amer. Chem. Soc.*, **81**, 549 (1959).
21. I. Bernal, J. Myrczek and J. Cetrullo, unpublished studies.
22. I. Bernal and J. Cetrullo, *Inorg. Chim. Acta*, **134**, 105 (1987).
23. I. Bernal, J. Cetrullo and S. Berhane, *Struct. Chem.*, **1**, 361 (1990).
24. M. Laing, S. Baines and P. Sommerville, *Inorg. Chem.*, **10**, 1057 (1971).
25. B. Nubert, H. Siebert, K. Weidenheimmer, J. Weiss and M.I. Ziegler, *Acta Crystallogr.*, **B35**, 1020 (1979).